UDK621.3:(53+54+621+66), ISSN0352-9045

ENLARGEMENT OF THE ROTATIONAL FIELD HOMOGENITY AREA IN A TWO-PHASE ROUND ROTATIONAL SINGLE SHEET TESTER

M. Jesenik, V. Goričan, M. Trlep, A. Hamler, B. Štumberger

Faculty of Electrical Engineering and Computer Science, University of Maribor, Maribor, Slovenia

Key words: magnetic devices, magnetic sheet, measurement, alternating magnetic fields, R.R.S.S.T., Round Rotational Single Sheet Testers, 3D modeling, three-dimensional modeling, calculations, numerical methods, FEM, Finite Element Method, experimental results

Abstract: Round rotational single sheet tester (R.R.S.S.T.) is used for the measurement of magnetic properties in rotational and alternating magnetic fields. The influence of the shields on the field homogeneity of the magnetic field distribution in the sample in the case of rotational magnetic field is investigated with finite element calculation. The aim of the calculation is to define optimal position of both side shields in order to expand the rotational field homogeneity area.

Povečanje področja homogenosti rotacijskega polja v dvofaznem rotacijskem merilniku magnetne pločevine

Ključne besede: naprave magnetne, pločevina magnetna, merjenje, polja magnetna izmenična, R.R.S.S.T. merilniki okrogli rotacijsko lastnosti pločevine magnetne enoslojne, modeliranje 3D tridimenzionalno, izračuni, metode numerične, FEM metoda elementov končnih, rezultati eksperimentalni

Izvleček: Okrogli merilec lastnosti magnetne pločevine se uporablja za merjenje lastnosti magnetne pločevine v rotacijskih in alternirajočih magnetnih poljih. Z izračuni, ki temeljijo na metodi končnih elementov, je proučevan vpliv ščitov na obliko rotacijskega polja v vzorcu okroglega merilca magnetne pločevine. Cilj izračunov je definiranje optimalne pozicije obojestranskih ščitov z namenom povečanja homogenega področja rotacijskega magnetnega polja.

1. Introduction

Two phase round rotational single sheet tester (R.R.S.S.T.) is used for the measurement of magnetic properties in rotational and alternating magnetic fields. Photo of the R.R.S.S.T. is shown in Fig. 1.

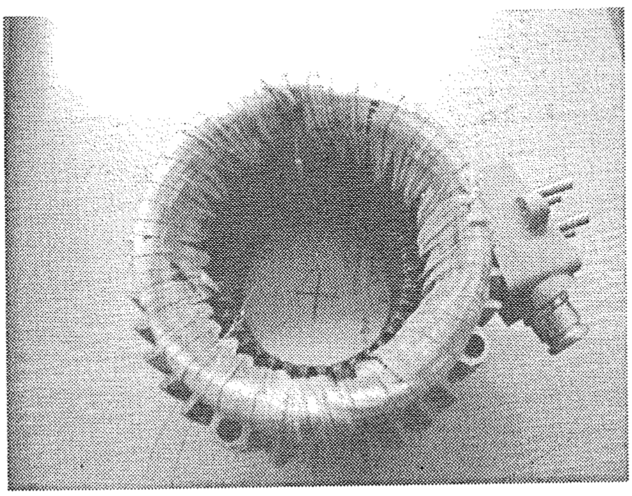

Fig. 1. Photo of the R.R.S.S.T.

The two phase winding is placed in the stator package of the induction motor and it produces rotational or alternating magnetic field. Measuring coils have to be placed in the homogeneous field. The excitation coils are longer than the sample thickness, which causes z-component of magnetic density $\boldsymbol{B}$ at the edges of the sample. The aim of the calculation is to define the optimal position of both side shields. The position of the shields can make the area of the homogeneous rotational field smaller or bigger than in the case with no shields by influencing the z-component of $\boldsymbol{B}$ /1/.

2. Modelling and calculation

R.R.S.S.T. is modelled as a 3D problem. The calculation is based on the use of the magnetic vector potential $\boldsymbol{A}$ and electric scalar potential V in the conducting area and only magnetic vector potential $\boldsymbol{A}$ in the nonconducting area ($\boldsymbol{A}$, V-$\boldsymbol{A}$ formulation /2/, /3/).

In the conducting area the differential Equations (1) and (2) have to be solved.

$$\nabla \times \frac{1}{\mu} \nabla \times A - \nabla \frac{1}{\mu} \nabla \cdot A + \sigma \frac{\partial A}{\partial t} + \sigma \nabla V = 0 \qquad (1)$$

$$\nabla \cdot \left(-\sigma \frac{\partial A}{\partial t} - \sigma \nabla V \right) = 0 \qquad (2)$$

In the nonconducting area the Equation (3) can be written.

$$\nabla \times \frac{1}{\mu} \nabla \times A - \nabla \frac{1}{\mu} \nabla \cdot A = J_s \tag{3}$$

σ is the conductivity of the material, μ is the permeability of the material and J_s is the excitation current.

The calculation is made as a nonlinear transient calculation (T.C.) /4/. Magnetic material is defined with magnetisation curve. Anisotropy of the material is not taken into account in the calculation.

Euler's method is used for the time integration. Potentials at the time instant $n+1$ are calculated as in (4).

$$\left(\mathbf{S} + \frac{\mathbf{T}}{\Delta t} \right) \cdot A^{(n+1)} = R^{(n+1)} + \frac{\mathbf{T}}{\Delta t} \cdot A^{(n)} \tag{4}$$

From (4) it is noticed that the potentials $A^{(n+1)}$ depend on the potentials from the previous time instant $A^{(n)}$. Euler's integration method is the first order integration method.

Cross sections of R.R.S.S.T. in the planes z=0 (horizontal plane) and x=0 (vertical plane) are shown in Fig. 2. and Fig. 3. separately. The length of the package is 86 mm. In Fig. 3. it can be seen, that d is the distance between the sample and the shield.

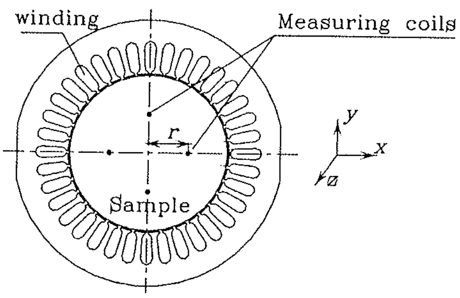

Fig. 2. R.R.S.S.T. in the plane z=0 (horizontal plane)

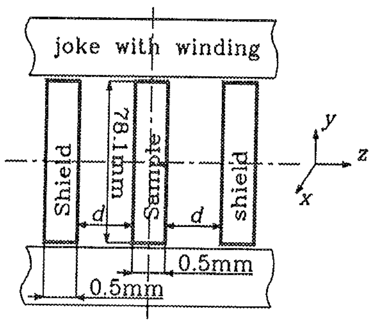

Fig. 3. R.R.S.S.T. in the plane x=0 (vertical plane)

Finite elements of the first order are used, which means that the approximation inside the element is linear. The elements are prisms. The two dimensional mesh of triangles in the horizontal plane is shown in Fig. 4. It is extracted into the three dimensional mesh of the prisms.

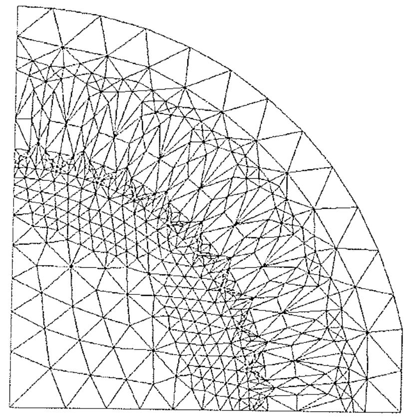

Fig. 4. Quarter of the 2D mesh in the horizontal plane

The problem is symmetrical. Only a half of the problem (from the centre z=0 to the end of the problem z=43 mm) is modelled and appropriate boundary conditions are set. The endings of the windings are not taken into account.

3. Results

The nonlinear characteristic of the material of the sample causes that the area of the homogeneous field is different for different $\boldsymbol{B}$ in the sample. If $\boldsymbol{B}$ in the centre of the sample is the same for all calculations, the nonlinearity of the material does not influence the result. Results are shown for magnetic density $\boldsymbol{B}$ = 1.43 T in the centre of the sample. The same can be concluded about the shields position influence on the field homogeneity for all amplitudes of $\boldsymbol{B}$. To get the same $\boldsymbol{B}$ in the centre of the sample algorithm from Fig. 5. is used.

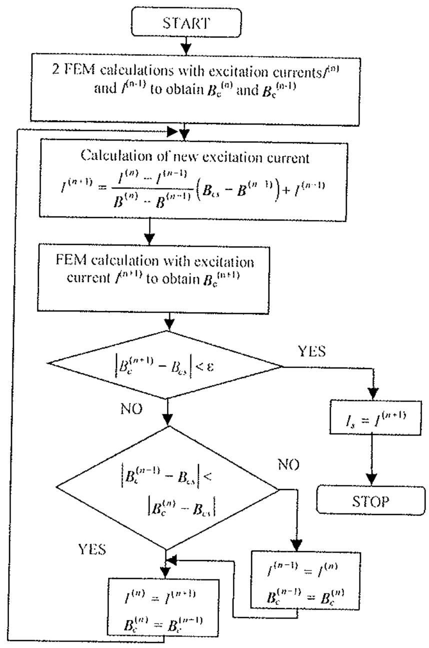

Fig. 5. Algorithm to get the same **B** *in the center of the sample.* $\mathbf{B}_{CS}$ *is* **B** *which we want to get in the center of the sample.* n-1, n, n+1 *are successive iterative calculation steps.*

The results obtained by use of both side shields are shown in Fig. 6. The procentual deviation of average value of $|\boldsymbol{B}|$ (averaging is made over the area enclosed by measuring coils) from value of $|\boldsymbol{B}|$ in the centre of the sample dependant on the radius of the measuring coils is shown.

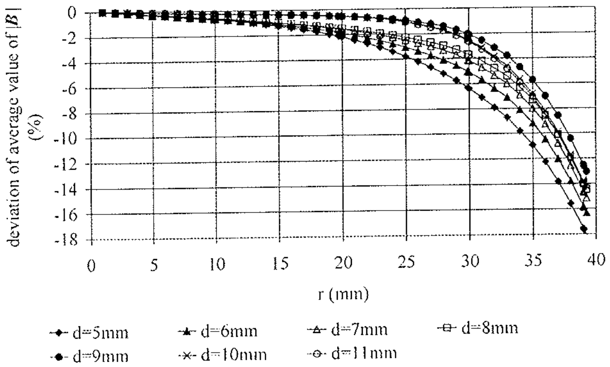

Fig. 6. Deviation of average value of |B| from the value of |B| in the centre of the sample dependant on the radius of the measuring coils

In Fig. 7., Fig. 8. and Fig. 9. magnetic flux density in the sample for the R.R.S.S.T. without the shields, for the R.R.S.S.T. with the shields which are in the distance of d = 5 mm from the sample and for the R.R.S.S.T. with the shields which are in the distance of d = 9 mm from the sample as in Fig. 3. is shown.

Z-component of $\boldsymbol{B}$ in the vertical plane for the R.R.S.S.T. without the shields, for the R.R.S.S.T. with the shields which are in the distance of d = 5 mm from the sample as in Fig. 3. and for the R.R.S.S.T. with the shields which are in the distance of d = 9 mm from the sample is shown in Fig. 10., Fig. 11., and Fig. 12. separately.

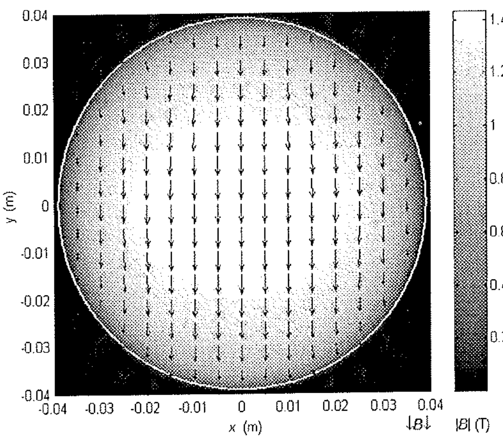

Fig. 7. B as arrows and as shading in the sample in the plane z = 0 for the rotational magnetisation direction at 270⁰ of 50 Hz T.C. for R.R.S.S.T. without the shields

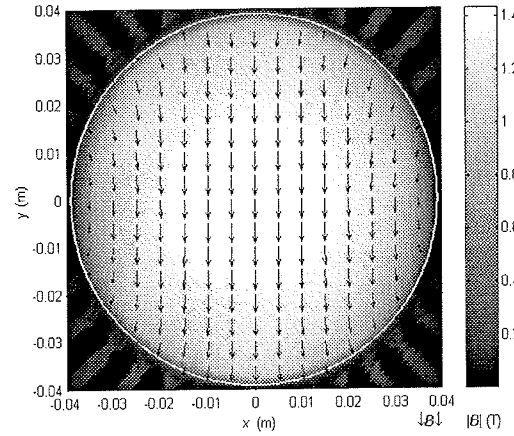

Fig. 8. B as arrows and as shading in the sample (z = 0) for the rotational magnetisation direction at 270⁰ of 50 Hz T.C. for R.R.S.S.T. with the shields (d = 5 mm)

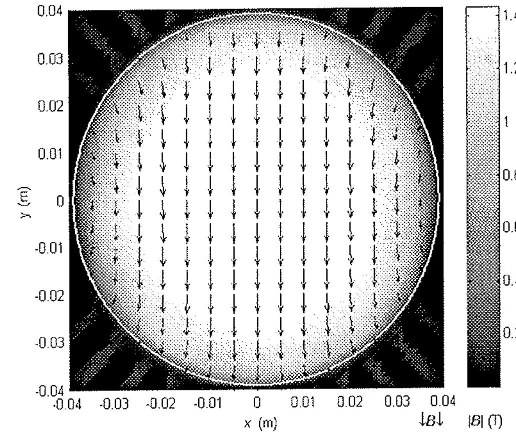

Fig. 9. B as arrows and as shading in the sample (z = 0) for the rotational magnetisation direction at 270⁰ of 50 Hz T.C. for R.R.S.S.T. with the shields (d = 9 mm)

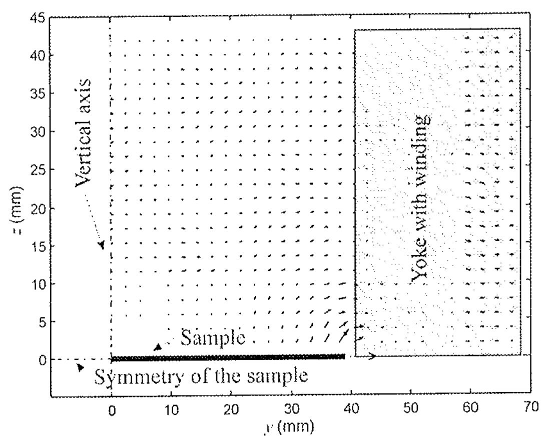

Fig. 10. B in the vertical plane for the rotational magnetisation direction at 270⁰ of 50 Hz T.C. for R.R.S.S.T. without the shields

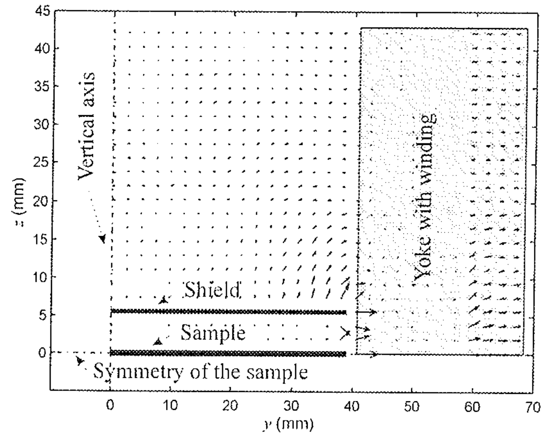

Fig. 11. **B** *in the vertical plane for the rotational magnetization direction at 270^0 of 50 Hz T.C. for R.R.S.S.T. with the shields (*d = 5 *mm)*

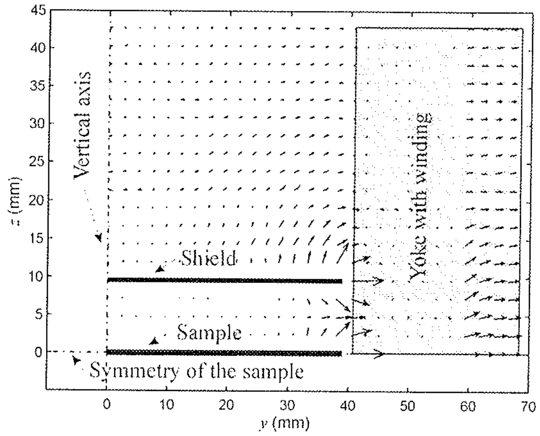

Fig. 12. **B** *in the vertical plane for the rotational magnetisation direction at 270^0 of 50 Hz T.C. for R.R.S.S.T. with the shields (*d = 9 *mm)*

In the case of T.C., the eddy currents appear at the edge of the sample and eddy currents cause that the direction of ***B*** in the sample does not coincide with the rotational magnetization direction. It can be seen from Fig. 13.

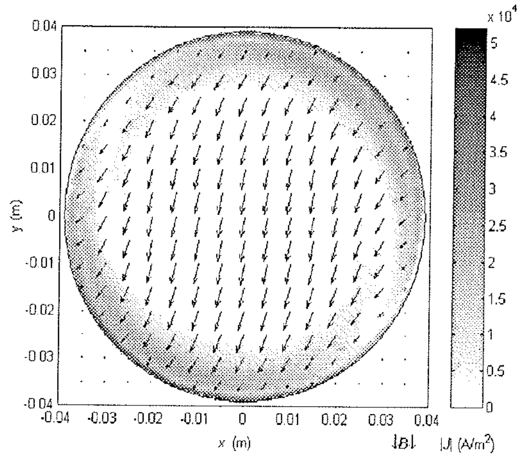

Fig. 13. **B** *as arrows and* **|J|** *as shading in the sample in the plane z=0 for the rotational magnetization direction at 270^0 of 500 Hz T.C.*

Fig. 14. shows changing of the direction of ***B*** depending on radius *r* of measuring coils for static calculation (S.C.), 50Hz transient calculation (T.C.) and 500Hz transient calculation. From Fig. 14. it can be seen that eddy currents in the case of 500Hz T.C. causes a big change of direction of ***B*** in the sample from the rotational magnetization direction. Shields improve only the amplitude of ***B*** but they do not influence the direction of ***B***. This is the reason why they are useful only for the frequencies in the rank of 50Hz.

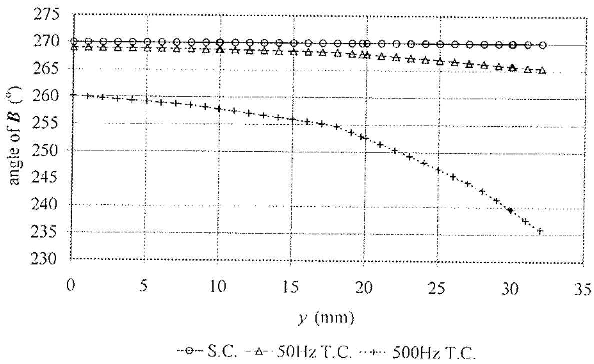

Fig. 14. Angle of **B** *along* y *axis for rotational magnetization direction at 270^0 of S.C., 50Hz T.C. and 500Hz T.C.*

Excitation currents obtained from the measurement on the N.O. 3% FeSi steel sample are used in the calculation. Procentual deviation between the 50Hz T.C. and measurement in the case where no shields are used for the rotational magnetization direction from 180^0 (t = 0 s) till 360^0 (t = 0.01 s) is shown in Fig. 15. Deviation is less than 9%. Deviation can be explained by the fact that anisotropy of the material and hysteresis effects are not taken into account in the calculation.

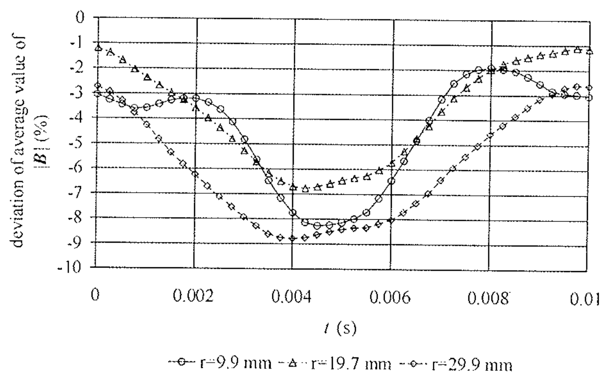

Fig. 15. Deviation of average value of **|B|** *for different* r *of measuring coils of 50Hz T.C. for R.R.S.S.T. without the shields from measurement*

4. Conclusions

The comparison of the best result for R.R.S.S.T. with both side shields and d = 9 mm, the result for R.R.S.S.T. with both side shields and d = 5 mm and result for R.R.S.S.T. with no shields is shown in Fig. 16. From Fig. 16. it can be seen that incorrect position of the shields can make the area of the homogeneous rotational filed smaller than in the case with no shields. The best result of all cases is obtained when both side shields are used and d = 9 mm.

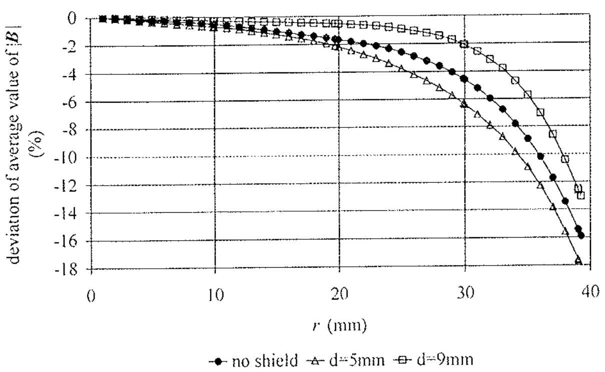

Fig. 16. Deviation of average value of |B| from the value of |B| in the centre of the sample dependant on the radius of the measuring coils

5. References

/1/ Dimitre Makaveev, Marc De Wulf, Jan Melkebeek, Field homogeneity in a two-phase rotational single sheet tester with square samples, Journal of Magnetism and Magnetic Materials 196-197 (1999) 937-939

/2/ O. Biro, K. Preis, On the Use of the Magnetic Vector Potential in the Finite Element Analysis of Three-Dimensional Eddy Currents, IEEE Transaction on Magnetics, Vol. 25, No. 4. pp 3145-3159, July 1989

/3/ Prolog to Eddy Currents: Theory and Applications, A tutorial introduction to the paper by Kriezis, Tsiboukis, Panas, and Tegopoulos, IEEE Proceedings, Vol. 80. No. 10, October 1992.

/4/ M. Trlep, B. Kreča, B. Hribernik, "Hybrid Finite Element - Boundary Method for Nonlinear Electromagnetic Problems", IEEE Transaction on Magnetics, Vol. 28. No.5. pp 2271-2273, September 1993

Marko Jesenik, Viktor Goričan, Mladen Trlep, Anton Hamler, Bojan Štumberger

Faculty of Electrical Engineering and Computer Science, University of Maribor, Smetanova 17, 2000 Maribor

Prispelo (Arrived):06.12.2001 Sprejeto (Accepted): 25.04.2002